

Energy spectrum and fluxes for Rayleigh Bénard convection

Pankaj Kumar Mishra¹ and Mahendra K. Verma¹

¹*Department of Physics, Indian Institute of Technology, Kanpur 208 016, India*

(Dated: February 6, 2020)

We compute the spectra and fluxes of the velocity and temperature fields in Rayleigh Bénard convection for a wide range of Prandtl numbers in turbulent regime using pseudo-spectral simulations on 512^3 grids. We adopt free-slip and conducting boundary condition for the simulations. Our spectral and flux studies support the Bolgiano-Obukhov scaling for high Prandtl number convection, and the Kolmogorov-Obukhov scaling for low Prandtl number and zero Prandtl number convection.

PACS numbers: 47.27.ek, 47.55.P-, 47.27.Gs, 47.55.pb

I. INTRODUCTION

Turbulent convection is one of the most challenging problems of classical physics [1]. A large number of work on convection have been done for an idealized version called Rayleigh Bénard convection (RBC) in which the fluid is heated between two parallel plates. The convective flow properties depend on two nondimensional parameters: the Rayleigh number (proportional to the buoyancy force) and the Prandtl number (the ratio of kinematic viscosity and thermal diffusivity). The convective flow becomes turbulent when the Rayleigh number is much larger than the critical Rayleigh number. One of the important topics in the study of convective turbulence is the scaling of energy spectra and energy fluxes of the velocity and temperature fields in the inertial range. In this paper we perform direct numerical simulation (DNS) and compute these quantities numerically and compare them with the existing phenomenologies.

The energy spectra and fluxes for convective turbulence are more complex than those for fluid turbulence due to the presence of the buoyancy force [2]. For stable stratified-fluid convection, Bolgiano [3] and obukhov [4] proposed dual cascade in the inertial range. For small wavenumbers (large length scale), they predicted dominance of buoyancy force over the inertial force leading to the velocity and temperature spectra as $k^{-11/5}$ and $k^{-7/5}$ respectively, where k is the wavenumber. In this regime, the flux for the temperature field is constant, while the flux of the velocity field varies as $k^{-4/5}$. For the intermediate wavenumbers, Bolgiano [3] and obukhov [4] conjectured dominance of the inertial force over the buoyancy force. Consequently the temperature field evolves as a passive scalar, and both the velocity and temperature fields have constant energy fluxes and $k^{-5/3}$ energy spectra [3, 4, 5]. The length scale that separates these two different regimes of energy cascades is called the ‘‘Bolgiano length’’ (l_B).

Later Procaccia and Zeitak [6], L’vov [7], and Falkovich and L’vov [8] proposed the same scaling for Rayleigh Bénard convection. In convective turbulence, for scales above the Bolgiano length ($l > l_B$), the kinetic energy spectrum ($E^u(k)$) and the entropy spectrum ($E^\theta(k)$) fol-

low the Bolgiano-Obukhov (BO) scaling

$$E^u(k) = C_k(\epsilon^\theta)^{\frac{2}{5}}(\alpha g)^{\frac{4}{5}}k^{-\frac{11}{5}}, \quad (1)$$

$$E^\theta(k) = C_\theta(\epsilon^\theta)^{\frac{4}{5}}(\alpha g)^{-\frac{2}{5}}k^{-\frac{7}{5}}, \quad (2)$$

$$\Pi^u(k) = C_f(\epsilon^\theta)^{\frac{3}{5}}(\alpha g)^{\frac{6}{5}}k^{-\frac{4}{5}}, \quad (3)$$

and for $l < l_B$, spectra follow Kolmogorov-Obukhov (KO) scaling

$$E^u(k) = K_{ko}(\epsilon^u)^{\frac{2}{3}}k^{-\frac{5}{3}}, \quad (4)$$

$$E^\theta(k) = K_\theta\epsilon^\theta(\epsilon^u)^{-\frac{1}{3}}k^{-\frac{5}{3}} \quad (5)$$

where Π^u is the kinetic energy flux, ϵ^u and ϵ^θ are the kinetic and entropy dissipation rate respectively, α is the thermal expansion coefficient of the fluid, and g is the acceleration due to gravity. Note that in literature, the spectrum and the flux of the temperature field are also referred to as the ‘‘entropy spectrum’’ and ‘‘entropy flux’’ respectively.

The Bolgiano length l_B has the following dependence on the convective parameters:

$$l_B = \frac{Nu^{\frac{1}{2}}d}{(RP)^{\frac{1}{4}}} \quad (6)$$

where Nu is the Nusselt number (dimensionless heat flux), R is the Rayleigh number, P is the Prandtl number, and d is the vertical height of the container. Grossmann and L’vov [9] argued that for $P < 1$, Bolgiano length is of the order of container’s size (see Eq. (6)). Hence, only KO scaling is expected in the inertial regime for low Prandtl number (low-P) convection. For large-Prandtl number (large-P) convection, l_B lies in the inertial regime, hence mixed scaling is expected.

Note that the above scaling arguments are applicable only to the bulk flow since they ignore the boundary layers. Shraimann and Siggia [10] and Grossmann and Lohse [11] incorporated the boundary layers and studied their effects on the heat transfers and scaling of various quantities.

There have been numerous experimental studies to test the above phenomenology of RB convection. Most convection experiments measured the velocity and temperature fields only at fixed locations of the apparatus. Taylor

frozen-turbulence hypothesis is assumed in these experiments. However, a small number of experiments measured high resolution spatial velocity and temperature fields for computing the above mentioned spectra. Experiments by Mashiko *et al.* [12] and sun *et al.* [13] belong to this category of experiments. Chilia *et al.* [14] and Cioni *et al.* [15] carried out convection experiments on water ($P \approx 7$) and mercury ($P \approx 0.02$) at large Rayleigh number, and found the frequency power spectrum to be consistent with BO scaling for water, and KO scaling for mercury. Heslot *et al.* [16] and Castaing [17] measured frequency power spectrum of the temperature field in He gas ($0.65 < P < 1.5$), and found the spectrum to be consistent with KO scaling. Wu *et al.* [18] however report BO scaling for Helium gas through frequency spectrum measurements of temperature. Zhou and Xia [19] and Shang and Xia [20] performed experiments on water and reported agreement with BO scaling. Askenazi *et al.* [21] and Mashiko *et al.* [12] reported BO scaling for SF₆ ($1 \leq P \leq 93$) and mercury respectively. Niemela *et al.* [22] measured temperature time series in He gas and reported the presence of both the KO and BO scaling. Thus the outcome of these experiments is not conclusive on the validity of the phenomenology of RB convection.

Numerical experiments provide important clues in turbulence. A series of numerical simulations of RB convection have been performed to test the KO and BO scaling. Grossmann and Lohse [23, 24] simulated RB fluid with $P = 1$ under Fourier-Weistrass approximation and reported KO scaling. Borue and Orszag [25] and Skandera *et al.* [26] performed pseudospectral simulation on $P = 1$ fluid with periodic boundary conditions on all directions and found consistency with KO scaling. Kerr [27] used pseudospectral method for his simulations of $P = 0.7$ fluid (air) under no-slip boundary conditions for the velocity and observed KO scaling. On the contrary, Cammusi and Verzicco [28] found agreement with the BO scaling in their simulation of $P = 0.7$ fluid in cylindrical geometry (finite difference method). These numerical results indicate uncertainty in the tests of the convective phenomenology.

Another way to investigate turbulent scaling is through the structure function calculations. Following Kolmogorov, Victor Yakhot [29] derived the exact analytical form of third order structure function for BO scaling in convective turbulence. Sun *et al.* [13] computed the structure function of the velocity and the temperature field in their convection experiment on water and reported KO scaling. Kunnen *et al.* [30] performed similar calculation on convection in water (both experiments and numerical simulation) and observed BO scaling. Calzavarini *et al.* [31] computed third-order structure function using Lattice Boltzmann method for $P = 1$ and reported BO scaling.

In this paper we compute the energy spectra and cascade rates for the velocity and temperature fields for a wide range of Prandtl number ($P = 0, 0.02, 0.2, 1, 6.8$) using numerical simulations. Our computations include

zero-P, low-P, and high-P convection, hence we have reasonable number of numerical runs to test the convective turbulence phenomenology. We adopt pseudo-spectral method and performed simulations on 512^3 grids using free-slip boundary conditions for the velocity field and conducting boundary condition for the temperature field. As a consequence of the above boundary conditions, the viscous boundary layer is absent, but the thermal boundary layer is present in our simulation. Hence we expect our simulation results to resemble somewhat with the convective patterns in the bulk.

The outline of the paper is as follows. Section II contains the dynamical equations and the definitions of the energy spectra and fluxes. The details and results of our numerical simulations is discussed in section III. We conclude in Sec. IV.

II. GOVERNING EQUATIONS

We numerically solve the nondimensionalized Rayleigh Bénard equations under Boussinesq approximation [32]

$$\frac{\partial \mathbf{u}}{\partial t} + (\mathbf{u} \cdot \nabla) \mathbf{u} = -\nabla \sigma + R\theta \hat{z} + \sqrt{\frac{P}{R}} \nabla^2 \mathbf{u}, \quad (7)$$

$$P \left(\frac{\partial \theta}{\partial t} + (\mathbf{u} \cdot \nabla) \theta \right) = u_3 + \sqrt{\frac{P}{R}} \nabla^2 \theta, \quad (8)$$

$$\nabla \cdot \mathbf{u} = 0 \quad (9)$$

where $\mathbf{u} = (u_1, u_2, u_3)$ is the velocity field, θ is the perturbations in the temperature field from the mean temperature, σ is the deviation of pressure from the conduction state, $R = \alpha g(\Delta T) d^4 / \nu \kappa$ is the Rayleigh number, $P = \nu / \kappa$ is the Prandtl number, and \hat{z} is the buoyancy direction. Here ν and κ are the kinematic viscosity and thermal diffusivity respectively, d is the vertical height of the container, and ΔT is the temperature difference between the plates. For the nondimensionalization we have used d as the length scale, $\sqrt{\alpha(\Delta T)gd}$ as the velocity scale, and $\nu(\Delta T)/\kappa$ as the temperature scale. For large-P convection, the temperature scale is taken as ΔT , and the governing equations is altered accordingly.

Zero Prandtl number (Zero-P) convection is the limiting case of low-P convection, and the corresponding dimensionless equations are

$$\frac{\partial \mathbf{u}}{\partial t} + (\mathbf{u} \cdot \nabla) \mathbf{u} = -\nabla \sigma + R\theta + \nabla^2 \mathbf{u}, \quad (10)$$

$$u_3 + \nabla^2 \theta = 0 \quad (11)$$

Here we use d as the length scale, ν/d as the velocity scale, and $\nu(\Delta T)/\kappa$ as the temperature scale.

Boundary conditions of the systems strongly affects the properties of the convective flow [11, 24]. We employ Free-slip and conducting boundary conditions on the horizontal plates, hence

$$u_3 = \partial_3 u_1 = \partial_3 u_2 = \theta = 0, \quad \text{at } z = 0, 1. \quad (12)$$

Periodic boundary conditions are applied along the horizontal directions. Viscous boundary layer is absent under the free-slip boundary conditions, however thermal boundary layers are present due to conducting boundary conditions. Hence our simulation results are expected to resemble the bulk flow due to the absence of the viscous boundary layer.

The energy spectrum for the velocity field $E^u(k)$ and the temperature fields $E^\theta(k)$ are defined as

$$E^u(k) = \sum_{k \leq k' < k+1} \frac{1}{2} |u(\mathbf{k}')|^2, \quad (13)$$

$$E^\theta(k) = \sum_{k \leq k' < k+1} \frac{1}{2} |\theta(\mathbf{k}')|^2. \quad (14)$$

Here the sum is being performed over the Fourier modes in the shell $(k, k+1)$. We will compute these spectra numerically at the steady state.

The energy flux is a measure of the nonlinear energy transfers in turbulence [33, 34, 35]. The energy flux for a given wavenumber sphere is the total energy transferred from the modes within the sphere to the modes outside the sphere. The energy flux has been studied in great detail for fluid and magnetohydrodynamic turbulence. However there are only a small number of work on the flux computations in convective turbulence [25, 26, 36]. Toh and Suzuki [36] defined the kinetic energy flux $\Pi_u(k_0)$ and the entropy flux $\Pi_\theta(k_0)$ based on Kraichnan formalism [37] as

$$\begin{aligned} \Pi^u(k_0) &= \frac{1}{2} \sum_{k > k_0} \sum_{p, q < k_0} \delta_{\mathbf{k}, \mathbf{p}+\mathbf{q}} i \frac{k_l k_m}{k_n} (1 - \delta_{l,n}) \\ &\quad \times u_l^*(\mathbf{k}) u_m(\mathbf{p}) u_n(\mathbf{q}) \end{aligned} \quad (15)$$

$$\begin{aligned} \Pi^\theta(k_0) &= \frac{1}{2} \sum_{k > k_0} \sum_{p, q < k_0} \delta_{\mathbf{k}, \mathbf{p}+\mathbf{q}} i (\mathbf{k} \cdot \mathbf{u}(\mathbf{q})) \\ &\quad \times (\theta^*(\mathbf{k}) \theta(\mathbf{p})) \end{aligned} \quad (16)$$

These quantities represent the net cascade of $|\theta|^2/2$ and $|\mathbf{u}|^2/2$ respectively from the modes within the wavenumber sphere of radius k_0 to the modes outside of the sphere.

The energy fluxes defined above can also be defined quite conveniently using the ‘‘mode-to-mode energy transfers’’ formalism that has been discussed in Verma [34]. According to this formalism, the kinetic energy flux and the entropy flux are

$$\Pi^u(k_0) = \sum_{k > k_0} \sum_{p < k_0} \delta_{\mathbf{k}, \mathbf{p}+\mathbf{q}} \Im([\mathbf{k} \cdot \mathbf{u}(\mathbf{q})][\mathbf{u}^*(\mathbf{k}) \cdot \mathbf{u}(\mathbf{p})]) \quad (17)$$

$$\Pi^\theta(k) = \sum_{k > k_0} \sum_{p < k_0} \delta_{\mathbf{k}, \mathbf{p}+\mathbf{q}} \Im([\mathbf{k} \cdot \mathbf{u}(\mathbf{q})][\theta^*(\mathbf{k}) \cdot \theta(\mathbf{p})]) \quad (18)$$

where \Im represents the imaginary part of the argument. We compute the spectra and fluxes of the velocity and temperature fields using numerical simulations [34]. These results will be described in the next section.

III. NUMERICAL SIMULATIONS AND RESULTS

As described in the previous section, the dynamical equations of RBC are Eqs. (7-8) for low-P convection and Eqs. (10-11) for zero-P convection. The equations for large-P convection are similar. We solve these equations numerically using pseudospectral method under free-slip and conducting boundary condition along the vertical (buoyancy) direction, and periodic boundary condition along the horizontal directions. We use Fourier basis for the horizontal directions. For the vertical direction, sine function is used for the vertical velocity and temperature fields, and cosine function is used for the horizontal velocity field.

The unidirectional initial energy and entropy spectra for the initial conditions are of the form:

$$E(k) = \frac{ak^4}{(k^4 + q^4)^{1+\alpha}} \exp(-bk^{1.1}), \quad (19)$$

where $b = 0.02$, $q = 1.5$, $\alpha = 2.8/12$, and a as a free parameter [38]. The initial phases are randomly generated. Time stepping of dynamical equations are carried out by fourth-order Runge-Kutta (*RK4*) scheme. We start our simulation on a smaller grid, and run the simulation until it reaches steady state. We then use the steady solution of the lower grid as an initial condition for a higher grid size at a higher R . We continue this procedure till turbulence state is reached. The final runs were performed on 512^3 grid for 20 large eddy turnover times on 8 nodes and 16 nodes of EKA, the supercomputer at Computational Research Laboratory. Zero-P convection runs were performed on 256^3 grid. The $k_{max}\eta$, where η is the Kolmogorov length, for our simulations are always greater than one. We choose five representative Prandtl numbers $P = 0, 0.02, 0.2, 1, 6.8$ for our spectra and flux studies. Our numerical results are discussed below.

A. Prandtl number $P = 6.8$

First we present the kinetic energy spectrum for $P = 6.8$ at $R = 6.6 \times 10^6$. In Fig. 1 we plot the compensated kinetic energy spectra $E^u(k)k^{5/3}$ (KO) and $E^u(k)k^{11/5}$ (BO). The flat region is rather short, yet, the BO line appears to be in a better agreement with the numerical results than the KO line. The inverse of Bolgiano length l_B^{-1} is around 16.4. Hence according to the convective turbulence phenomenology discussed in Section I, the BO scaling should hold for $k < l_B^{-1}$, and the KO scaling should hold for $k > l_B^{-1}$. The BO scaling appears to be present in our numerical results, but the KO scaling is not observable. The dominance of dissipation for modes with $k > l_B^{-1}$ in our 512^3 simulation may be the reason for the absence of the KO scaling. We need higher resolution simulation to investigate this issue.

Fig. 2 exhibits entropy spectrum that contains two distinct spectra. A careful observation shows that the

upper spectral curve corresponds to the Fourier modes $\theta_{002}, \theta_{004}, \theta_{006}, \dots$ (here the three indices are k_x, k_y , and k_z respectively). Paul *et al.* [39] studied these modes for free-slip and conductive boundary conditions, and showed using phenomenological arguments that $\theta_{002} \approx 1/(2\pi) \approx -0.15$ independent of Prandtl number. Our numerically computed θ_{002} and corresponding spectrum $E_\theta(k = 2\pi)$ are in very good agreement with the prediction of Paul *et al.* The Fourier modes $\theta_{004}, \theta_{006}$ and θ_{008} are also larger than other Fourier modes that form the lower energy spectrum curve. This is the reason for the existence of dual entropy spectral curves.

The modes $\theta_{002}, \theta_{004}, \theta_{006}, \dots$ maintain their energy, and they do not participate in nonlinear energy transfers. Thus the entropy flux appear to be generated by the modes of the lower spectral curve, We compare the lower curve with the BO and KO scaling. Among the two, the BO scaling fits better with the numerical data than the KO scaling. Note that the dual spectra for entropy is a consequence of free-slip boundary condition, and it is absent in no-slip and periodic boundary conditions simulations.

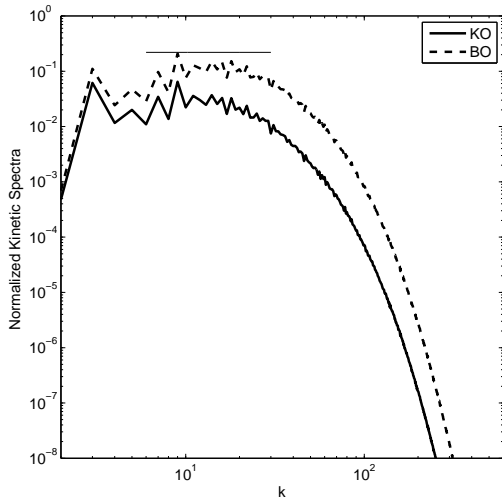


FIG. 1: Plot of the compensated kinetic energy spectra $E^u(k)k^{5/3}$ (KO) and $E^u(k)k^{11/5}$ (BO) vs. k for $P = 6.8$, $R = 6.6 \times 10^6$ on 512^3 grid. The horizontal line indicates an agreement with the BO scaling for large- P convection.

We complement our spectral analysis with energy flux studies. Recall that for large- P convection, under the BO scaling, the entropy flux is constant but the energy flux varies as $k^{-4/5}$ (see Eq. (3)). In contrast, the fluxes of the kinetic energy and entropy are constant in the KO scaling. In Fig. 3 we plot both the fluxes as well as the compensated kinetic energy flux $\Pi^u(k)k^{4/5}$. We observe that entropy flux as well as the compensated kinetic energy flux are constant in the inertial range. The range of the kinetic energy flux is rather small, but the entropy flux is a constant for a significantly large wavenumber range. Note that $\Pi^u(k)$ falls rather steeply as a function

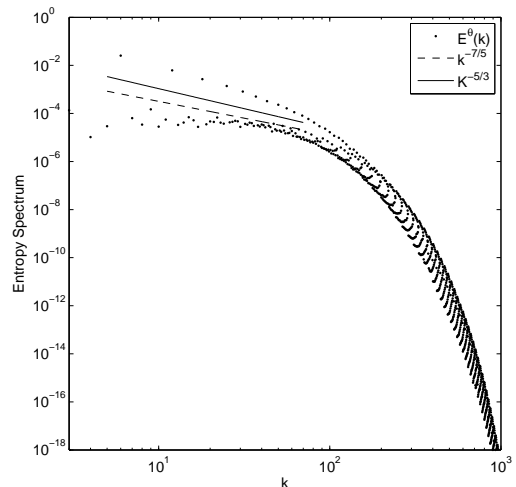


FIG. 2: Plot of entropy spectrum $E^\theta(k)$ vs. k for $P = 6.8$, $R = 6.6 \times 10^6$ on 512^3 grid. The lower part of the spectrum matches reasonably well with $k^{-7/5}$ line.

of wavenumbers.

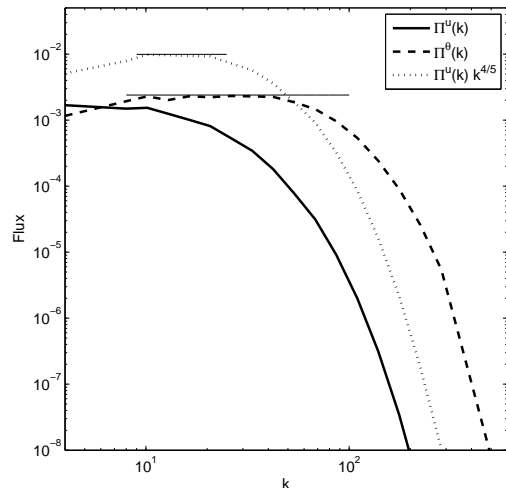


FIG. 3: Plot of the kinetic energy flux (solid line) and the entropy flux (dashed line) vs. k for $R = 6.6 \times 10^6$, $P = 6.8$ on 512^3 grid. The normalized kinetic energy flux (multiplied by $k^{4/5}$) is also shown in the figure as a dotted line. The flux results are in better agreement with the BO scaling than the KO scaling.

From these observations we conclude that for large- P convection, the BO scaling is a better model than the KO scaling.

B. Prandtl number $P = 1$

Next we present the kinetic energy and entropy spectra and fluxes for $P = 1$ at $R = 6.6 \times 10^6$. Figs. 4 and

5 exhibit the compensated kinetic energy spectra and entropy spectrum respectively. The kinetic energy spectrum is in a better agreement with the KO scaling than the BO scaling, a result consistent with earlier work by Borue and Orszag [25] and Skandera *et al.* [26].

The entropy spectrum, shown in Fig. 5, has two distinct slopes similar to $P = 6.8$ case. In agreement with the predictions of Paul *et al.* [39], the values of θ_{002} and its corresponding entropy spectrum E^θ (the upper curve in Fig. 5) are similar to those for $P = 6.8$. Comparison of the lower curve with BO or KO scaling yields somewhat ambiguous results, and it is difficult to ascertain which of the two scaling works for the entropy spectrum. Fig. 6 shows the kinetic energy and entropy fluxes along with the compensated kinetic energy flux. Here, the KO scaling appears to be a better fit than the BO scaling.

The spectra and flux results for $P = 1$ indicate a transition from the BO scaling to the KO scaling. $P = 1$ is probably the dividing Prandtl number between the large- P and the small- P convection regimes.

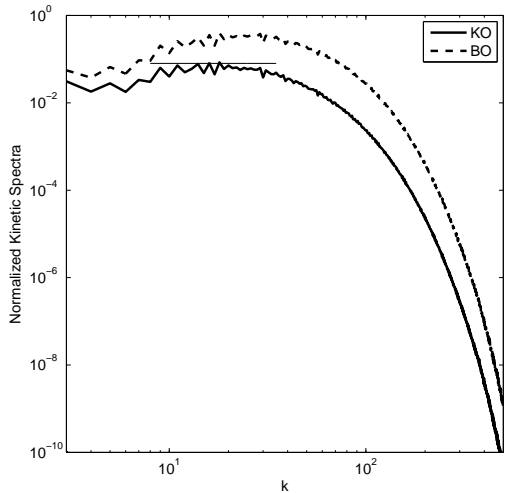


FIG. 4: Plot of the compensated kinetic energy spectra $E^u(k)k^{5/3}$ (KO) and $E^u(k)k^{11/5}$ (BO) vs. k for $R = 6.6 \times 10^6$, $P = 1$ on 512^3 grid.

C. Prandtl number $P = 0.2$

Next we present our numerical results for $P = 0.2$ at $R = 6.6 \times 10^6$. In Fig. 7 we plot the compensated kinetic energy spectra $E^u(k)k^{5/3}$ (KO) and $E^u(k)k^{11/5}$ (BO). The inertial range is between $k = 20 - 80$, and the inverse of the Bolgiano length is around 0.01. Hence we do not expect to observe the BO scaling. Even though both the BO and the KO scaling do not fit very well with the numerically computed energy spectrum, yet the KO scaling is in better agreement with the numerical data than the BO scaling.

In Fig. 8 we plot the entropy spectrum. We obtain bi-spectra similar to that for $P = 6.8$ and $P = 1$. The

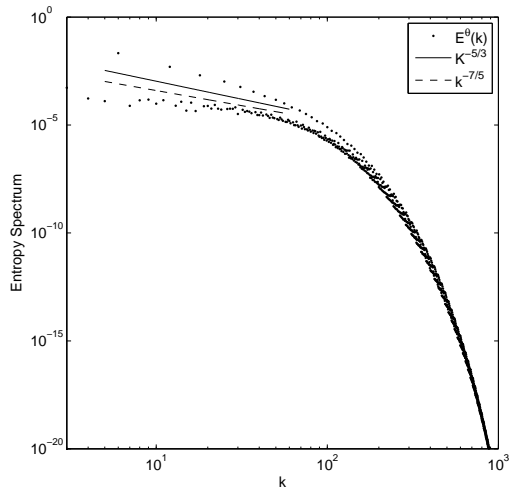


FIG. 5: Plot of the entropy spectrum vs. k for $R = 6.6 \times 10^6$, $P = 1$ on 512^3 grid.

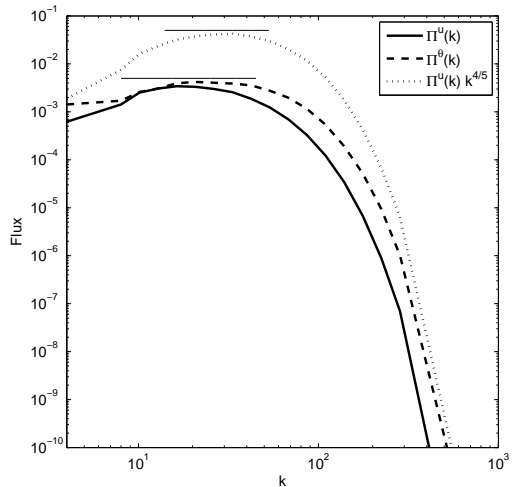


FIG. 6: Plot of the kinetic energy flux (solid line) and the entropy flux (dashed line) vs. k for $R = 6.6 \times 10^6$, $P = 1$ on 512^3 grid. The dotted line represents $\Pi^u(k)k^{4/5}$ curve. The kinetic energy and entropy fluxes are constant in the narrow inertial range indicating agreement with the KO scaling for $P = 1$.

upper curves represent the spectrum of the Fourier modes $\theta_{002}, \theta_{004}, \theta_{006}, \dots$ etc. The lower curve however appears to fit better with the KO scaling than the BO scaling.

Next, we compute the energy fluxes for the velocity and temperature fields for the same run. Inset of Fig. 7 shows the velocity and entropy fluxes. We observe constant fluxes for both the velocity and temperature fields. Given the kinetic energy spectrum and flux, we compute Kolmogorov's constant using Eq. (4) that yields $K_{Ko} \approx 2.0$ with significant error. Considering the uncertainties in the numerical fits, this value is in a reasonable agreement with Kolmogorov's constant for the fluid or the passive-

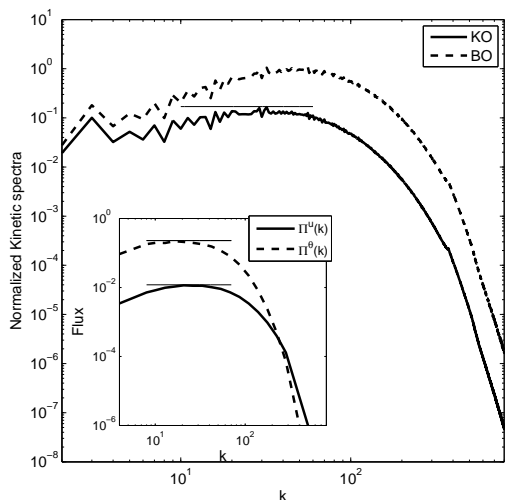


FIG. 7: Plot of the compensated kinetic energy spectra $E^u(k)k^{5/3}$ (KO) and $E^u(k)k^{11/5}$ (BO) vs. k for $R = 6.6 \times 10^6$, $P = 0.2$ on 512^3 grid. The numerical results match better with the KO scaling than the BO scaling. In the inset the kinetic energy flux (solid line) and the entropy flux (dashed line) are plotted for the same parameters; they are constant indicating an agreement with KO scaling.

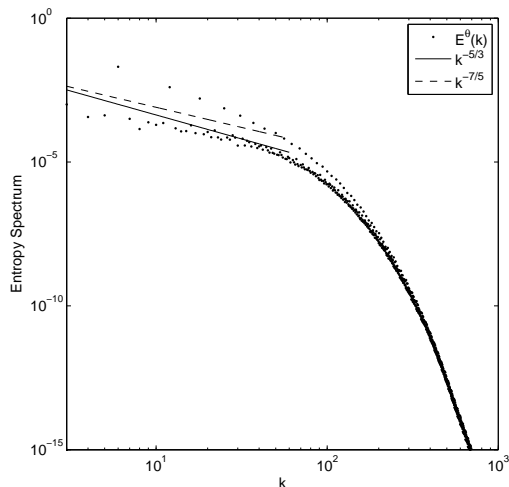


FIG. 8: Plot of the entropy spectrum vs. k for $R = 6.6 \times 10^6$, $P = 0.2$ on 512^3 grid. Here the KO scaling matches better with the numerical data.

scalar turbulence measured earlier using experiments and numerical simulations.

Thus for $P = 0.2$, the numerical values of kinetic energy and entropy spectra and fluxes fit better with the predictions of the KO scaling than the BO scaling.

D. Prandtl number $P = 0.02$

Now we compute the kinetic energy and the entropy spectra and fluxes for $P = 0.02$ at $R = 2.6 \times 10^6$. Fig. 9 contains the compensated kinetic energy spectra for the KO and BO scaling. Neither the KO spectrum nor the BO spectrum matches with the numerically computed kinetic energy spectrum, yet the KO scaling fits better with the numerical data than the BO scaling. Fig. 10 contains the numerically computed entropy spectrum. The KO scaling appears to fit better with the lower curve of the figure than the BO scaling. As discussed earlier, the upper curve corresponds to $\theta_{0,0,2n}$ Fourier modes.

The inset of Fig. 9 shows the energy and entropy fluxes. The kinetic energy flux is flat for more than a decade, but the range of constant entropy flux is rather small. The entropy flux tends to decay due to the large thermal diffusivity.

On the whole, the numerical results for $P = 0.02$, which is a representative of low-P convection, appear to favour KO scaling than BO scaling. In the next subsection we compute kinetic energy spectrum and flux for $P = 0$, which is an asymptotic case for low-P convection.

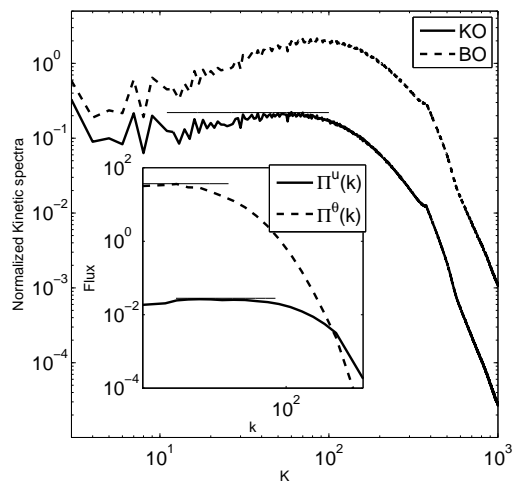


FIG. 9: Plot of the compensated kinetic energy spectra $E^u(k)k^{5/3}$ (KO) and $E^u(k)k^{11/5}$ (BO) vs. k for $R = 2.6 \times 10^6$, $P = 0.02$ on 512^3 grid. Both the KO and the BO scaling do not fit well with the numerically computed spectrum, yet, the KO scaling is in better agreement than BO scaling. The kinetic energy flux (solid line) and the entropy flux (dashed line) are plotted in the inset.

E. Prandtl number $P = 0$

For $P = 0$, the temperature fluctuations can be expressed as $\theta(\mathbf{k}) = u_3(\mathbf{k})/k^2$ using Eq. (11). Consequently $E^\theta(k) \approx E^u(k)/k^4$. Hence the entropy spectrum is very steep for zero-P convection, and we can safely assume

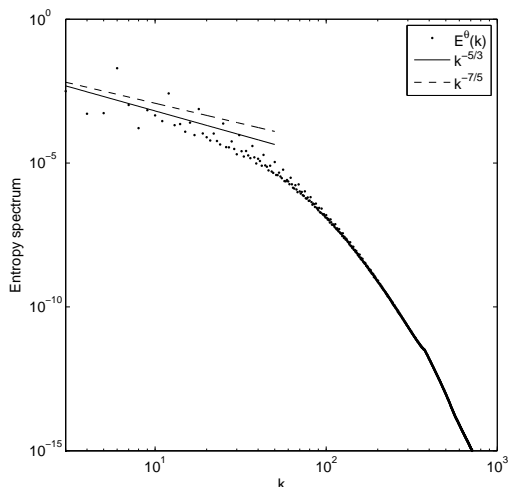


FIG. 10: Plot of the entropy spectrum for $R = 2.6 \times 10^6$, $P = 0.02$ on 512^3 grid. The DNS spectrum is in better agreement with KO scaling than BO scaling.

that the velocity field is buoyantly forced only at very large scales (small k). Hence, Kolmogorov's argument for the fluid turbulence must be valid for zero-Prandtl number convection. This argument closely resembles mathematical derivation of Spiegel [40].

We performed DNS for $P = 0$ at $R = 1.97 \times 10^4$, and computed the energy spectrum using the steady-state data. The compensated kinetic energy spectrum thus computed is illustrated in Fig. 11 that clearly exhibits the KO scaling, thus verifying the above arguments. Using simulation data we also compute kinetic energy flux that is plotted in the inset of Fig. 11. The kinetic energy flux is flat in the inertial range, thus it is in agreement with the KO scaling. The Kolmogorov constant for $P = 0$ is around 1.8 (with the significant errors) which is in a reasonable agreement with the expected value of 1.6 (Kolmogorov's constant for the fluid turbulence).

IV. CONCLUSIONS

We numerically compute the kinetic energy and entropy spectra and fluxes of convective turbulence using pseudospectral method. We performed these simulations for a large range of Prandtl numbers—zero-P, low-P, and high-P. The Rayleigh number of our simulation is around a million, which is at the lower end of turbulent convection.

Our numerical results show that the phenomenology of large-P convection is closer to the Bolgiano-Obukhov (BO) scaling than the Kolmogorov-Obukhov (KO) scaling. Here, the kinetic energy spectrum $E^u(k) \sim k^{-11/5}$, and the entropy spectrum $E^\theta \sim k^{-7/5}$. The kinetic energy flux $\Pi^u(k) \sim k^{-4/5}$, while the entropy flux Π^θ is a constant. Thus for large-P convection, the buoyancy

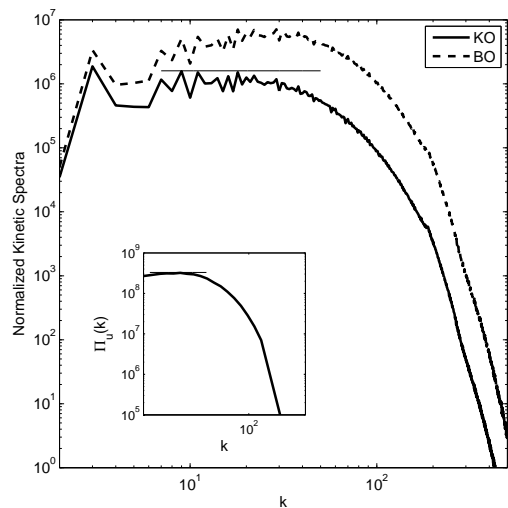


FIG. 11: Plot of the compensated kinetic energy spectra $E^u(k)k^{5/3}$ (KO) and $E^u(k)k^{11/5}$ (BO) vs. k for $R = 1.97 \times 10^4$, $P = 0$ on 256^3 grid. The DNS spectrum matches with KO spectrum quite well. The kinetic energy flux, plotted in the inset, is constant showing consistency with KO scaling.

force dominates the inertial force. In these simulations we have not observed the signature of coexistence of both the KO and BO scaling because the wavenumbers beyond l_B^{-1} (inverse of Bolgiano length) appear to be dissipated strongly thus making the observation of KO regime rather difficult.

For low-P convection ($P \leq 1$) convection, our numerical results are in better agreement with the KO scaling than the BO scaling. In these runs, $E^u(k) \sim k^{-5/3}$, $E^\theta \sim k^{-5/3}$, $\Pi^u(k) \sim const$, and $\Pi^\theta(k) \sim const$. Hence, the buoyancy force appears to be an irrelevant variable in renormalization group sense, and the temperature field is advected by the velocity field similar to that in passive scalar turbulence. Also, BO scaling is not observable for low-P convection runs because l_B^{-1} is too small.

For zero-P convection, we observe KO scaling for the velocity field ($E^u(k) \sim k^{-5/3}$ and $\Pi^u(k) \sim const$) rather conclusively. The temperature field is active only for very small wavenumbers since $E^\theta(k) \sim E^u(k)/k^4$. Hence, the buoyancy force is active only for small wavenumbers leading to Kolmogorov's scaling just like in fluid turbulence.

We observe that sometimes our computational grid of 512^3 is not sufficient to resolve the scaling (BO or KO). We need to go up to 1024^3 or higher grids, which is very expensive at present. We also need to perform runs similar to those presented here for no-slip and periodic boundary conditions to isolate the effects of the boundary layers.

Acknowledgements: We thank Krishna Kumar, Supriyo Paul, and Stephan Fauve for valuable discussions and suggestions. We thank Computational Research Laboratories (CRL) for providing access to the supercomputer EKA where the above simulations were

performed. This work was supported by funds from Department of Science and Technology, India as Swarna-

jayanti fellowship to MKV.

-
- [1] G. Ahlers, S. Grossmann, and D. Lohse, *Rev. Modern Phys.* **81** (2009).
- [2] E. D. Siggia, *Annu. Rev. Fluid Mech.* **26**, 137 (1994).
- [3] R. Bolgiano, *J. Geophys. Res.* **64**, 2226 (1959).
- [4] A. M. Obukhov, *Dokl. Akad. Nauk SSSR* **125**, 1246 (1959).
- [5] A.N. Kolmogorov, *Dokl. Akad. Nauk SSSR* **32**, 16 (1941).
- [6] I. Procaccia and R. Zeitak, *Phys. Rev. Lett.* **62**, 2128 (1989).
- [7] V. S. L'vov, *Phys. Rev. Lett.* **67**, 687 (1991).
- [8] G. Falkovich and V.S. L'vov, *Physica D* **57**, 85 (1992).
- [9] S. Grossmann and V.S. L'vov, *Phys. Rev. E* **47**, 4161 (1993).
- [10] B.I. Shraiman and E.D. Siggia, *Phys. Rev. A* **42**, 3650 (1990).
- [11] S. Grossmann, D. Lohse, *J. Fluid Mech.* **407**, 27 (2000).
- [12] T. Mashiko, Y. Tsuji, T. Mizuno, and M. Sano, *Phys. Rev. E* **69**, 036306 (2004).
- [13] C. Sun, Q. Zhou, and K. Q. Xia, *Phys. Rev. Lett.* **97**, 144504 (2006).
- [14] F. Chilia, S. Ciliberto, C. Innocenti, and E. Pampaloni, *Nuovo Cimento D* **15**, 1229 (1993).
- [15] S. Cioni, S. Ciliberto and J. Sommeria, *Euophys. Lett.* **32**, 413 (1995).
- [16] F. Heslot, L. Kadanoff, A. Libchaber, S. Thomae, X. Z. Wu, S. Zaleski, and G. Zanetti, *J. Fluid Mech.* **204**, I (1989).
- [17] B. Castaing, *Phys. Rev. Lett.* **65**, 3209 (1990).
- [18] X.Z. Wu, L. Kadanoff, A. Libchaber, and M. Sano, *Phys. Rev. Lett.* **64**, 2140 (1990).
- [19] S.Q. Zhou and K.Q. Xia, *Phys. Rev. Lett.* **87**, 06451 (2001).
- [20] X. D. Shang and K. Q. Xia, *Phys. Rev. E* **64**, 065301 (2001).
- [21] S. Askenazi and V. Steinberg, *Phys. Rev. Lett.* **83**, 4760 (1999).
- [22] J.J. Niemela, L. Skrbek, K.R. Sreenivasan and R. J. Donnelly, *Nature (London)* **404**, 837 (2000).
- [23] S. Grossmann and D. Lohse, *Phys. Rev. Lett.* **67**, 445 (1991).
- [24] S. Grossmann, and D. Lohse, *Phys. Rev. A* **46**, 903 (1992).
- [25] V. Bourue and S. A. Orszag, *Journal of Sci. Computing* **12**, 305 (1997).
- [26] D. Skandera, A. Busse, W.C. Muller, High Performance computing in science and engineering, Transactions of the Third joint HLRB and KONWIHR status and result workshop, Springer Berlin, Part **IV**, 387 (2008).
- [27] R. M. Kerr, *J. Fluid Mech.* **310**, 139 (1996).
- [28] R. Camussi, R. Verzicco, *European Journal Of Mechanics B*, **23**, 427 (2004).
- [29] V. Yakhot, *Phys. Rev. Lett.* **69**, 769 (1992).
- [30] R. P. Kunnen, H.J.H. Clecx, B.J. Geruts, L.J.A.V. Bokhoven, R.A.D. Akkermans, and R. Verzicco, *Phys. Rev. E* **77**, 016302(2008).
- [31] E. Calzavarini, F. Toshi, R. Tripiccion, *Phys. Rev. E* **66**, 016304 (2002).
- [32] O. Thual, *J. Fluid Mech.* **240**, 229 (1992).
- [33] M. Lesieur, *Turbulence in fluids*, Kluwer Acc. Publishers, (1990)
- [34] M. K. Verma, *Phys. Rep.* **401**, 229 (2004).
- [35] R. Kraichnan, *J. Fluid Mech.* **5**, 497 (1959).
- [36] S. Toh and E. Suzuki, *Phys. Rev. Lett.* **73**, 1501 (1994).
- [37] R. H. Kraichnan, *Phys. Fluids*, **8**, 1385 (1965).
- [38] O. Debliquy, M. K. Verma and D. Carati, *Phys. of Plasmas* **12**, 042309 (2005).
- [39] S. Paul, P.K. Mishra, M. K. Verma, and K. Kumar, arXiv:0904.2917 (2009)
- [40] E. A. Spiegel, *J. Geophys. Res.* **67**, 3063 (1962).